JCTC Journal of Chemical Theory and Computation

Article

pubs.acs.org/JCTC

On Atomistic and Coarse-Grained Models for C_{60} Fullerene

Luca Monticelli*

INSERM, UMR-S665, Paris, F-75015, France

Université Paris Diderot, Sorbonne Paris Cité, UMR-S665, Paris, F-75013, France

INTS, Paris, F-75015, France

ABSTRACT: Many atomistic and coarse-grained simulations of fullerene and fullerene derivatives are reported in the literature, but validation of both atomistic and coarse-grained models has been very limited. Here, we report a thorough validation of several all-atom fullerene models and refinement of the MARTINI coarse-grained (CG) fullerene model. The all-atom model by Girifalco had been parametrized using only solid-state properties (lattice constant, heat of sublimation), but it performs well also in the liquid state in terms of partitioning between different solvents. The new MARTINI CG model is optimized by matching experimental free energies of transfer between different solvents (for fullerene−solvent interactions) and atomistic fullerene−fullerene potentials of mean force (PMF) in water and in octane (for fullerene−fullerene interactions). The model gives reasonable results for solid-state properties and also reproduces atomistic results on the PMF in a lipid membrane. We conclude that the new MARTINI model is suitable for large-scale simulations of the interaction of fullerene with water, organic solvents, and lipid membranes.

INTRODUCTION

Since their discovery in 1985,[1] fullerenes have attracted much attention for their unique properties. For example, their remarkable electron acceptor ability makes them suitable components of donor−acceptor complexes for artificial photosynthesis.[2] Numerous applications have been described for fullerene in several areas of science and technology, and particularly in the field of photovoltaic devices.[3] Applications in biomedical sciences have also been proposed, mostly related to fullerene high permeability through biological barriers,[4] its capability to entrap metals and small molecules,[5] and its antioxidant properties.[6] Endohedral metallofullerenes, in which metal ions are trapped inside the fullerene cage, have been proposed as powerful contrast agents for magnetic resonance imaging.[5]

Simulations of fullerenes and carbon nanotubes at different levels have been carried out since the early 1990s. Quantum mechanics calculations have been used to predict, among others, electronic and structural properties.[7,8] Classical simulations have been used to study fullerene interactions with water and other solvents (reviewed in ref 9). The results of classical simulations depend critically on the potential energy functions used to represent the molecule, and on the properties used as a target in the force field parametrization. In the specific case of fullerene, a large number of atomistic simulations has been published in the literature. However, little work has been done to validate the potentials used, and few papers have been published with comparisons between results from atomistic simulations and experimental data.[9] Rivelino and co-workers compared the free energy of transfer of fullerene between different solvents for six different fullerene parametrizations, showing significant differences among the models.[10] While free energies of transfer are of fundamental importance to assessing the interaction of fullerene with different solvents, they do not contain information on the interaction of fullerene with other fullerene molecules—in other words, on the cohesive forces that are present in the solid phase or in solid-like aggregates (e.g., clusters in solution).

Large-scale behavior of fullerene has been explored using coarse-grained (CG) simulations.[11−14] Again, little work has been done to validate coarse-grained potentials. CG studies on the aggregation behavior of fullerene yielded different and sometimes contrasting results.[11,13] Those results clearly depend on the force field employed and will reproduce the experimental behavior only if both fullerene−solvent and fullerene−fullerene interactions are carefully calibrated.

In the present study, we compare and validate both atomistic and coarse-grained models for fullerene. The manuscript is divided into two parts: first, we present an assessment of the quality of four atomistic force fields currently in use, with particular emphasis on two models; second, we optimize the MARTINI coarse-grained (CG) force field for fullerene. The performance of atomistic force fields is assessed by comparing (a) the partitioning behavior, as a stringent test for fullerene−solvent interactions, and (b) the enthalpy of sublimation, a measure of the cohesive forces in the solid. Refinement of the MARTINI CG model for fullerene is based on the simultaneous optimization of several quantities, including experimental partitioning coefficients, sublimation energies, and fullerene−fullerene potentials of mean force in water and alkanes.

METHODS

The validation of atomistic models relies on the comparison between experimental and calculated thermodynamic quantities. In the following paragraphs, we describe, for both the atomistic and the coarse-grained models, (1) the force fields, (2) the simulation parameters, and (3) the different method-

Received: January 6, 2012
Published: March 8, 2012

dx.doi.org/10.1021/ct3000102 | J. Chem. Theory Comput. 2012, 8, 1370−1378

ologies used to calculate thermodynamic properties. (Force field and structure files are available free of charge on the Web sites http://www.dsimb.inserm.fr/~luca/ and http://md.chem.rug.nl/cgmartini/.)

All-Atom Fullerene Models. We used four different all-atom models of fullerene, all sharing identical bonded interactions but with four different sets of nonbonded (van der Waals) interactions. In all models, partial charges on all atoms were set to zero. Bond lengths for the atomistic model were taken from experimental NMR data.[15] Bonded force constants were taken from the OPLS-AA force field[16] (values for the aromatic carbons). Lennard-Jones (LJ) parameters were chosen from models that have already been used for fullerene in the literature: (1) the model developed by Girifalco, who used the enthalpy of sublimation and the lattice parameter of solid C_{60} crystals to derive LJ parameters;[17,18] (2) the model of Rivelino et al.[10,19] [in both cited works, the authors claim to be using LJ parameters from OPLS-AA, without specifying the atom type chosen; in fact, their parameters are similar to those for benzene carbon and for alkene carbon but do not correspond exactly to either one of them]; (3) the models used by Qiao et al.,[20,21] with parameters from the GMX force field;[22] and (4) the model used by Levitt et al.,[23] with parameters from the benzene carbon in OPLS-AA (atom type 145).[16]

All-Atom Simulation Parameters. Most simulation parameters were identical in all atomistic simulations. The force field for all organic solvents (octane, tridecane, acetone, 1-butanol, and ethanol) was OPLS-UA;[24] the water model was SPC.[25] All simulations of condensed phases used a cutoff of 1.0 nm for nonbonded interactions. The usual correction for long-range dispersion interactions[26] was used in simulations of isotropic systems (as required with OPLS force fields) but not for membrane systems. The particle mesh Ewald (PME) algorithm[27,28] was used in all atomistic systems for the calculation of long-range electrostatic interactions, with a fourth order spline interpolation and a 0.12 nm grid spacing. We used the stochastic dynamics integrator in all calculations, with an inverse friction coefficient of 1 ps. In calculations of enthalpies of sublimation and free energy of transfer, we used no constraints on fullerene and on solvents, and a time step of 1 fs. In calculations of the potential of mean force, we used SETTLE[29] to constrain water bonds and LINCS[30,31] for all of the bonds in octane and in the membrane; in this case, the time step was 2 fs. All simulations in the NPT ensemble were carried out with the Parrinello–Rahman barostat[32] (time constant of 4 ps, compressibility of 4.5×10^{-5}, pressure of 1 bar) at the temperature of 298 K (unless stated otherwise). In the case of membrane simulations, semi-isotropic pressure coupling was applied, with the box vector along the bilayer normal coupled separately from those in the membrane plane; time constants, compressibilities, and pressures were the same as for simulations in isotropic solvents. All simulations were carried out with the GROMACS software package (v4.5).[33,34]

All-Atom Models: Enthalpies of Sublimation. We calculated enthalpies of sublimation from simulations of solid fullerene crystals and from gas phase simulations, using

$$\Delta H_{\text{sublimation}} = (U_{\text{gas}} + pV_{\text{gas}}) - (U_{\text{solid}} + pV_{\text{solid}}) \approx U_{\text{gas}} - U_{\text{solid}} + RT \quad (1)$$

where U_{gas} and U_{solid} are the total energies (per mole) of the gas and solid phase respectively, p indicates the pressure, V_{gas} and V_{solid} indicate the molar volume of the gas and the solid, R is the universal gas constant, and T is the absolute temperature. The pV_{solid} term is negligible and therefore omitted. For solid crystal simulations, we used the experimental structure of fullerene crystals (that is, face-centered cubic, FCC) as a starting configuration in all cases. At 300 K, the fullerene FCC crystal has a lattice constant of 1.417 nm (ref 35). The simulation box consisted of 256 fullerene molecules ($4 \times 4 \times 4$ unit cells). Simulations of solid crystals were carried out for 20 ns, using the simulation parameters detailed above. Only the last 10 ns were used for analysis. Simulations in the gas phase were performed in the NVT ensemble (298 K) with the stochastic dynamics integrator (inverse friction coefficient of 1 ps), using a single fullerene molecule in a large empty box ($8 \times 8 \times 8$ nm). No constraints were used. The time step was 1 fs, and the total simulation time was 50 ns.

All-Atom Models: Free Energy of Transfer. In simulations, the free energy of transfer can be calculated from the difference in the free energy of solvation:

$$\Delta G_{\text{transfer}} = \Delta G_{\text{solvation1}} - \Delta G_{\text{solvation2}} \quad (2)$$

Free energies of solvation were calculated using the thermodynamic integration (TI) technique, using the well-known formula:[36]

$$\Delta G = \int_{\lambda=0}^{\lambda=1} \left\langle \frac{\partial H(\lambda)}{\partial \lambda} \right\rangle_{\lambda} \mathrm{d}\lambda \quad (3)$$

For each solvent, a series of 23 simulations was performed with values of λ from 0 to 1. The λ values were not equally spaced and not identical in each simulation: smaller spacing was used where the slope of the $\mathrm{d}G/\mathrm{d}\lambda$ curve changed more rapidly. Since C_{60} has no partial charges, there was no need to decouple electrostatic and Lennard-Jones interactions separately.

A soft-core potential was used for the nonbonded interactions to avoid the singularity in the potential when the interactions were turned off.[37] The soft-core parameter α, which controls the height of the potential around $r = 0$, was set to 0.65. The soft-core power was set to 1, and the range of the interaction (soft-core σ) was set to 0.3 nm. All other simulation parameters were the same as detailed above.

One problem arises when the decoupling cage molecules in solvents consisting of small molecules: the solvent may get "trapped" inside the cage, causing instability and artifacts in the calculations. [We were not able to solve the problem above simply by varying soft-core parameters or other simulation parameters. We find it surprising that other authors have not reported similar problems in their TI calculations on fullerene, especially in the case of small solvent molecules like ethanol and water.] To avoid this problem, we carried out the TI calculations in three steps, using a modified topology containing one virtual atom in the center of the cage. The virtual atom has no mass, and its position is calculated at every step from the center of mass of the fullerene molecule. All interactions of the virtual atom with the fullerene cage are set to zero, but the particle can interact with the solvent. In the first step of the TI simulation, we calculated the free energy change upon coupling the central atom to the solvent system. We then calculated the free energy change for coupling the rest of the molecule to the solvent. No solvent can get trapped inside the cage, due to the presence of the virtual atom. Finally, we

decoupled the virtual atom from the solvent. Summing up the contributions from the three steps, the interaction of the virtual atom with the solvent cancels out.

For each value of λ, the simulation time was 1 ns for the first step, 8 ns for the second, and 2 ns for the third, for a total simulation time of 11 ns × 23 = 253 ns for each solvent. Error estimates on the free energy derivative were calculated by block averaging,[26] while the error on the integral was calculated using standard error propagation rules.

Atomistic Simulations: Potential of Mean Force. We performed potential of mean force (PMF) calculations on fullerene dimers in water and octane using the umbrella sampling technique[38] and the weighted histogram analysis method (WHAM).[39] A series of simulations was performed in which two fullerene molecules were restrained at a given distance from each other using a harmonic potential, with a force constant of 3000 kJ mol^{-1} nm^{-2}. The distance between the two fullerenes was increased from 0.9 to 2.9 nm with 0.1 nm increments. After equilibrating for 5 ns, each simulation was 100 ns long, for a total simulation time of 2.1 μs (production only) for each PMF calculated in water and in octane. Simulations were carried out in the NPT ensemble at 313 K with isotropic pressure coupling. Constraints were applied to all bonds in calculations of potentials of mean force, using the same algorithms and parameters as detailed above. All other simulation parameters were as specified above. A snapshot of the dimer system set up in water is shown in Figure 1.

The PMF of fullerene as a function of the distance from the center of a POPC lipid bilayer was calculated using a similar methodology. Parameters for the lipids were taken from the work of Berger et al.;[40] the water model was SPC.[25] The simulation box contained a single C_{60} molecule, 72 lipids, and 4226 water molecules. The z component of the distance between the center of mass of fullerene and that of the POPC membrane was restrained with a harmonic potential (force constant: 1000 kJ mol^{-1} nm^{-2}) at distances between 0 and 4.5 nm with 0.1 nm increments. Each simulation consisted of 10 ns of equilibration (not used in the analysis) and 200 ns of production run, for a total (production) simulation time of 9.2 μs. The statistical uncertainty in all umbrella sampling simulations was evaluated using the bootstrap analysis implemented in GROMACS.[41]

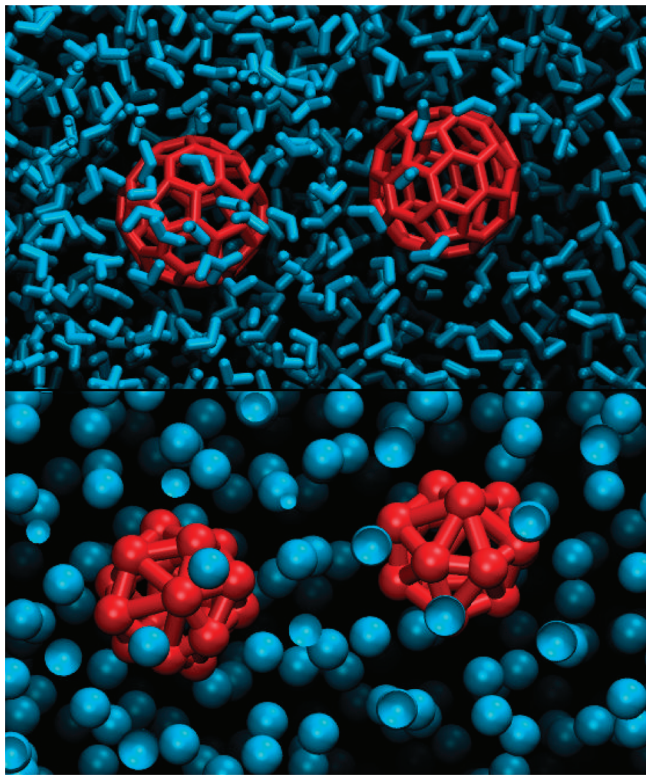

Figure 1. Snapshots from all-atom (top) and coarse-grained (bottom) simulations of fullerene dimers in water.

Coarse-Grained Fullerene: Building the Models. The original MARTINI CG fullerene model, developed in our previous work,[11] is consistent with the MARTINI coarse-grained force field for lipids,[42,43] proteins,[44] carbohydrates,[45] and various polymers.[46−48] In the MARTINI force field, approximately four non-hydrogen atoms are represented by a single interaction site (4:1 mapping), except in the case of ring structures, where mapping is approximately 2:1. The fullerene original model[11] consisted of 16 beads; in the present work, we also tested an alternative model with 20 particles. The particles were placed on a spherical surface and the interparticle distances were maximized. We tested diameters of 0.68 nm, 0.70, and 0.72 nm. All of the particles were then connected with an elastic network of bonds, with a force constant of 1250 kJ mol^{-1} nm^{-2}.

Coarse-Grained Fullerene: Simulation Parameters. Simulation parameters were the standard ones used with the MARTINI force field. Nonbonded interactions were calculated with a cutoff of 1.2 nm. A shift function was applied for electrostatic interactions from 0 nm and for LJ interactions from 0.9 nm. Electrostatic interactions were scaled with a dielectric constant of 15. All simulations in the NPT ensemble were carried out at 298 K, using the stochastic dynamics integrator (inverse friction coefficient of 1 ps), the Parrinello−Rahman barostat[32] (time constant of 5 ps, compressibility of 4.5 × 10^{-5}, pressure of 1 bar), and no constraints. All CG simulations were performed with the GROMACS software package (v4.0.7 and v4.5.3).[33,34]

We used a time step of 20 fs in all CG simulations, unless specified otherwise. Throughout the paper, we report only the formal simulation time, without any conversion factor.

Coarse-Grained Simulations: Free Energy of Transfer. The free energies of transfer between different solvents were derived from free energies of solvation, calculated with thermodynamic integration formula (see above). For each solvent, a series of 23 simulations was performed with values of λ from 0 to 1. Like in atomistic simulations, the λ values were not equally spaced and not identical in each simulation: smaller spacing was used close to the steepest points in the $dG/d\lambda$ curve. Each simulation was equilibrated for 10 ns, and the production runs were 400 ns long. A soft-core potential was used for the nonbonded interactions to avoid the singularity in the potential when the interactions were turned off.[37] The soft-core parameter α was set to 1.3. The soft-core λ power was set to 1, and the range of the interaction (soft-core σ) was set to 0.47 nm. These values are optimized for the MARTINI CG model and allow solvent molecules to overlap with solute beads at values of λ around 0.5. Simulations were carried out in the NPT ensemble (298 K, 1 bar) using isotropic pressure coupling.

Coarse-Grained Simulations: Enthalpy of Sublimation. The enthalpy of sublimation was calculated with the same procedure as for the atomistic model. We built FCC fullerene

crystals using the experimental value of the lattice constant and simulated the crystals for 500 ns in the NPT ensemble (temperature of 298 K, pressure of 1 bar, isotropic pressure coupling). Simulations in the gas phase were performed in the NVT ensemble (298 K) with the stochastic dynamics integrator (same procedure as in the corresponding atomistic simulations). The time step was 10 fs, both in the solid and in the gas phase, and no constraints were applied.

Coarse-Grained Simulations: Potential of Mean Force. The potential of mean force (PMF) was calculated for fullerene dimers following the same methodology as in the atomistic simulations. Twenty-one simulations were carried out with fullerene−fullerene distances restrained at distances between 0.9 and 2.9 nm, using a harmonic potential with force constant of 1000 kJ mol^{-1} nm^{-2}. Simulations were performed in the NPT ensemble at 313 K (same temperature as in atomistic simulations), with isotropic pressure coupling (1 bar). Sampling was 1 μs per umbrella potential (total simulation time: 21 μs for each PMF). A snapshot of the dimer system set up in water is shown in Figure 1.

The PMF of fullerene as a function of the distance from the center of a POPC lipid bilayer was calculated using the same methodology. The simulation box contained one fullerene, 128 lipids (64 per leaflet), and 1500 water molecules. Semi-isotropic pressure coupling was used. The distance between the center of mass of fullerene and that of the POPC membrane was restrained with a harmonic potential (force constant: 1000 kJ mol^{-1} nm^{-2}) at distances between 0 and 4.5 nm with 0.1 nm increments. Each simulation was 1 μs long, for a total simulation time of 46 μs. As in atomistic simulations, the statistical uncertainty in all umbrella sampling simulations was estimated using the bootstrap analysis implemented in GROMACS.[41]

RESULTS

Validating All-Atom Fullerene Models: Enthalpies of Sublimation and Free Energies of Transfer. The enthalpy of sublimation is an important thermodynamic property providing a measure of cohesive forces in the solid state. We calculated this property for four different fullerene models. Results are reported in Table 1.

The most widely accepted experimental measures for fullerene enthalpy of sublimation range between 176 and 183 kJ/mol.[49,50] As expected, the closest agreement with the experimental values is obtained with the Girifalco model, which was parametrized to reproduce both crystal lattice parameters and the heat of sublimation.[17,18] The Rivelino et al. and OPLS-AA force fields give reasonable values for both the enthalpy of sublimation and the lattice constant, although they both overestimate the cohesive interactions in the solid by more than 10%. The GMX force field severely overestimates both the heat and the lattice constant. In all cases, deviations appear to be largely due to the Lennard-Jones parameters (larger ε and σ). On the basis of these results, and considering the high computational cost of free energy calculations, we decided to explore further the thermodynamic properties of only two out of four models: the one by Girifalco and the one by Rivelino et al..

Table 1. Enthalpies of Sublimation and Lattice Constants for Face-Centered Cubic (FCC) Fullerene Crystals, in Experiments and Simulations with Four Different Force Fields[a]

	experiment	Girifalco	Rivelino et al.	GMX	OPLS-AA (145)
LJ σ (nm)		0.3469	0.3500	0.3741	0.3550
LJ ε (kJ/mol)		0.2764	0.3180	0.5026	0.2929
ΔHsublimation (kJ/mol)	180 ± 3	178.4 ± 0.3	211.6 ± 0.4	402.8 ± 0.4	201.9 ± 0.3
lattice constant (nm)	1.417	1.417 ± 0.0004	1.419 ± 0.0004	1.442 ± 0.0003	1.425 ± 0.0003

[a]Lennard-Jones parameters for each model are also reported. For OPLS-AA, atom type 145 was used.[16]

Free energies of transfer of the fullerene between different solvents are not available directly from experiments, but they can be derived from solubilities, which are available from experiments. The use of solubilities relies on the assumption that, to a first approximation, the free energy of solution can be decomposed into two main contributions: the free energy of sublimation (to take a mole of solute from the solid phase to the gas phase) and the free energy of solvation (to take one mole of solute from the gas phase to the solution).

$$\Delta G_{solution} = \Delta G_{sublimation} + \Delta G_{solvation} \quad (4)$$

Free energies of sublimation are independent of the solvent; therefore, in principle, the solubility depends mainly on the free energy of solvation. If this approximation is valid, the free energy of transfer between two solvents can be calculated simply from

$$\begin{aligned}\Delta G_{transfer} &= \Delta G_{solvation1} - \Delta G_{solvation2} \\ &= \Delta G_{solution1} - \Delta G_{solution2} \\ &= -RT \ln(x_1/x_2)\end{aligned} \quad (5)$$

where x_1 and x_2 are the solubilities in solvents 1 and 2 expressed as molar fractions. Experimental free energies derived with the approximations above are calculated from solubility data in ref 51 and reported in Table 2.

The free energies of transfer between different solvents are reported in Table 2 for two different fullerene models, Girifalco and Rivelino et al.

It is clear from Table 2 that the performance of the two force fields is quite similar and that both are in reasonable agreement with experimental data. Girifalco's model performs better than Rivelino et al.'s, with an average unsigned error (calculated as the average unsigned difference between calculated and experimental values) of 4.5 kJ/mol versus 6.2 kJ/mol (excluding the results for water, for which the solubility data is less reliable than for other solvents). Since the Girifalco model gives the best agreement with experimental data both in terms of partitioning and sublimation, we use it as a reference in the refinement and validation of the coarse-grained MARTINI potential.

MARTINI Coarse-Grained Model: Optimization. We optimized the original MARTINI fullerene model[11] through a trial-and-error procedure, aiming at reproducing several quantities at the same time: (1) the free energy of transfer of fullerene between different solvents, based on experimental results; (2) the fullerene−fullerene interaction energy, as calculated by fullerene−fullerene potential of mean force calculations in polar and nonpolar phases; and (3) the enthalpy of sublimation, as measured experimentally. In order to reproduce all of these quantities, we followed a procedure

Table 2. Free Energies of Transfer of Fullerene between Different Solvents, in Experiments and Simulations Carried out with Two Different Atomistic Force Fields[a]

experiments				
ΔG_transfer (kJ/mol)	octane	acetone	1-butanol	ethanol
octane				
acetone	6.56			
1-butanol	7.25	0.70		
ethanol	13.95	7.39	6.69	
water	96.67	90.11	89.42	82.73
Girifalco				
ΔG_transfer (kJ/mol)	octane	acetone	1-butanol	ethanol
octane				
acetone	2.55			
1-butanol	4.4	1.85		
ethanol	17.89	15.34	13.49	
water	91.81	89.26	87.41	73.92
Rivelino et al.				
ΔG_transfer (kJ/mol)	octane	acetone	1-butanol	ethanol
octane				
acetone	1.16			
1-butanol	2.27	1.11		
ethanol	19.3	18.14	17.03	
water	96.1	94.94	93.83	76.8

[a]The statistical uncertainty is less than 0.5 kJ/mol in all simulations.

that can be ideally split into four parts: (1) determination of the number of interaction sites (mapping), (2) determination of bonded parameters, (3) determination of Lennard-Jones parameters for the fullerene−solvent interaction, and (4) determination of Lennard-Jones parameters for the fullerene−fullerene interaction.

CG models were built by placing a number of beads (16 or 20) on the surface of a sphere at the maximum possible distance from each other. The radius of the sphere was varied, and fullerene−fullerene PMFs were calculated in water for each model and compared to atomistic results. The position of the negative peak in the PMF depends mostly on the fullerene size (i.e., on the radius of the sphere). The best match was obtained for a sphere of radius 0.35 nm.

The choice of the number of beads was based on the enthalpy of sublimation. Models with 20 coarse-grained beads (3:1 mapping) overestimated the heat of sublimation approximately by a factor of 2 compared to experimental results (360−380 kJ/mol, depending on the precise choice of the Lennard-Jones parameters). The large mismatch is due mainly to the high symmetry of the model, which has the geometry of an ideal dodecahedron and packs very well in the FCC crystal (high number of close contacts in the crystal). Models with 16 beads (approximately 4:1 mapping) have a less regular shape and pack less well in the crystal, which results in heats of sublimation much closer to the experimental value (210−220 kJ/mol).

Nonbonded interactions between the fullerene and different solvents were optimized on the basis of experimental partitioning of the fullerene between six organic solvents: benzene, octane, cyclohexane, acetone, 1-butanol, and ethanol. Free energies of transfer into water were also calculated, but they were not used as a target in the parametrization because of the high uncertainty in the experimental measures. Lennard-Jones parameters in MARTINI cannot be calculated via combination rules, and each parameter has to be determined separately. The benzene particle type (SC4) was used as a starting point in the refinement procedure. The majority of fullerene−solvent interaction parameters had to be modified—although, usually the changes were rather small. Results on partitioning are reported in Table 3.

Parameters for fullerene−fullerene interaction were determined on the basis of fullerene dimer PMFs in water and in octane, obtained from atomistic models with the Girifalco model. Again, the interaction between benzene particles (SC4−SC4) was used as a starting point, and the Lennard-Jones interaction parameter (epsilon) had to be slightly modified (with a trial-and-error procedure) to obtain the best match between atomistic and coarse-grained results. The PMFs for atomistic and coarse-grained simulations are reported in Figure

Table 3. Free Energy of Transfer of MARTINI Fullerene between Different Solvents[a]

experiments						
AG_transfer (kJ/mol)	benzene	octane	cyclohexane	acetone	1-butanol	ethanol
benzene						
octane	8.6					
chyclohexane	12.1	3.5				
acetone	15.2	6.6	3.1			
1-butanol	15.9	7.3	3.8	0.7		
ethanol	22.5	13.9	10.4	7.4	6.7	
water	105.3	96.7	93.2	90.1	89.4	82.7
MARTINI						
ΔG_transfer (kJ/mol)	benzene	octane	cyclohexane	acetone	1-butanol	ethanol
benzene						
octane	10.1					
chyclohexane	12.9	2.7				
acetone	14.5	4.4	1.7			
1-butanol	18.4	8.2	5.5	3.8		
ethanol	23.1	12.9	10.2	8.5	4.7	
water	85.5	75.3	72.6	70.9	67.1	62.4

[a]The statistical uncertainty is less than 0.1 kJ/mol in all cases.

2. Using 2.1 μs of total sampling in atomistic simulations, the statistical uncertainty in the free energy minimum at contact is

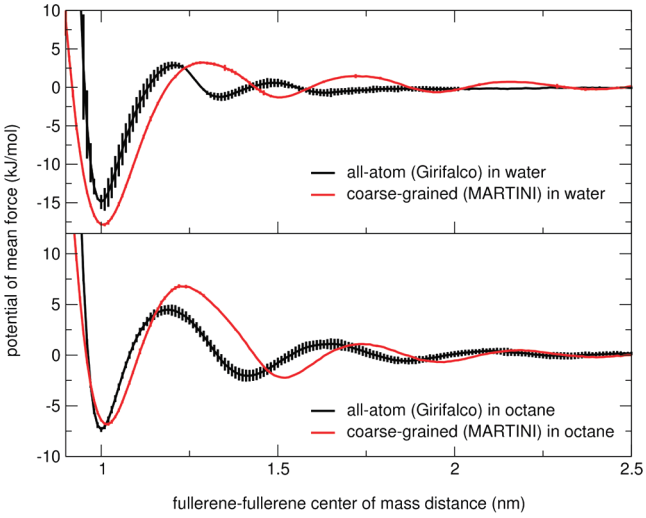

Figure 2. Potential of mean force for fullerene–fullerene interaction in water (top) and octane (bottom), from atomistic and coarse-grained simulations. Error bars represent the statistical uncertainty and are reported in all graphs (they are barely visible for the CG calculations thanks to much longer sampling).

reduced to about 0.9 kJ/mol in water and 0.1 kJ/mol in octane; uncertainties in CG calculations are much smaller, thanks to longer sampling. The correspondence between atomistic and CG profiles is satisfactory, although not perfect. The free energy gain upon dimerization was overestimated in water by 2.9 kJ/mol in water and underestimated by 0.5 kJ/mol in octane. Also, both CG profiles show a series of local minima that are either not present or more shallow in atomistic profiles. These local minima appear to be artifacts of the CG model.

MARTINI Fullerene: Validation. In order to validate the new CG MARTINI model, we calculate the PMF for a single fullerene as a function of the distance from the center of a bilayer membrane. Similar calculations have been already reported in the literature using different force fields for fullerene, the lipids, and water.[12,13,21,52] Here, we repeat the calculations using the Girifalco model for fullerene, the Berger force field for POPC lipids, and the SPC water model. A sampling time of 200 ns per umbrella (total simulation time of 9.2 μs) was necessary to reduce the statistical uncertainty to around 2 k_BT. Again, CG simulations achieve much smaller statistical error due to longer sampling (1 μs per umbrella, total simulation time of 46 μs) and faster dynamics of the membrane. Results are reported in Figure 3.

Two main differences are evident from the comparison of the two PMFs. The first one is the presence of a small barrier to fullerene penetration in the CG simulation, not observed in the atomistic simulation. The second is a shift in the position of the free energy minimum from about 0.8 nm from the bilayer center (in the atomistic representation) to about 1.15 nm (in the CG representation). The slope of the PMF is very similar in the two representations, as well as the depth of the minimum and the free energy of the system with fullerene in the center of the membrane. Overall, the agreement between the atomistic and CG profiles is satisfactory.

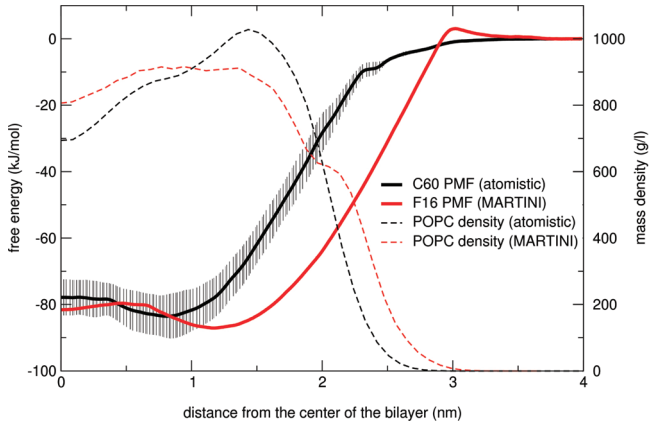

Figure 3. PMF for a system with a single fullerene and a POPC bilayer, as a function of the distance between their centers of mass. Error bars represent the statistical uncertainty and are reported only for the atomistic simulation, as for the CG simulation they are comparable to the thickness of the line. Dashed lines represent mass density profiles of the POPC membrane, in atomistic and CG simulations.

DISCUSSION

Girifalco determined Lennard-Jones parameters for fullerene carbon in 1992, using the heat of sublimation as a target property.[18] Not surprisingly, Girifalco's parameters yield indeed excellent agreement with experimental measures in the solid state. The other three models tested in the present work[20,23,53] overestimate the fullerene heat of sublimation, mostly due to larger values of the Lennard-Jones ϵ parameter. We emphasize that Lennard-Jones parameters used in the literature for fullerene were "borrowed" from standard carbon atom types used in force fields for biological macromolecules and were neither derived from fullerene properties nor validated by comparison with experimental data on fullerene. It is therefore not surprising that they perform worse than Girifalco's parameters. The difference in heat of sublimation between the Girifalco model and the other three models tested is expected to influence all properties that depend on fullerene–fullerene cohesive forces, and therefore the aggregation behavior. For example, it is likely that the other models will overestimate the free energy change upon dimerization in all solvents, and therefore the tendency of fullerene to aggregate.

While the Girifalco model performs very well in terms of solid-state properties, few tests had been reported on its performance in solution. We used free energies of transfer as a criterion for validating atomistic parameters for two reasons: first, partitioning between different solvents is important for determining molecular interactions in a complex chemical environment (such as a lipid membrane); second, partitioning was used as a target property in the development of our CG model, and in the MARTINI force field in general. Rivelino and co-workers followed a similar approach in testing several fullerene models[10] but used only two solvents. In the present work, we used four solvents and achieved higher precision thanks to our three-step thermodynamic integration procedure and to longer sampling.

For atomistic simulations of fullerene in different solvents, we used Lennard-Jones parameters simply obtained via geometric combination rules. Both the Girifalco and the Rivelino et al. models give reasonable agreement with solubility-derived partitioning data. Because the OPLS-AA

dx.doi.org/10.1021/ct3000102 | J. Chem. Theory Comput. 2012, 8, 1370–1378

benzene atom type (atom type 145) has Lennard-Jones parameters quite similar to those of the two atom types above, we expect it to provide reasonable fullerene−solvent interactions and partitioning. On the other hand, we expect the GMX force field to give significantly different partitioning behavior. This intuitive view is corroborated by results on fullerene PMF in DPPC membranes, showing an energy gain upon fullerene permeation much lower than reported here for the Girifalco model.[21]

Some authors[52,54] have used modifications of the Girifalco model, where the Lennard-Jones parameters for carbon−oxygen interactions were taken from the work of Werder et al., who parametrized those interactions on the basis of the graphite−water contact angle.[55] Werder et al.'s parameters provide interactions that are less attractive than those obtained by combination rules. [Werder et al.'s parameters: σ_{C-O} = 0.319 nm, ε_{C-O} = 0.392 kJ/mol; geometric combination rules: σ_{C-O} = 0.331 nm, ε_{C-O} = 0.424 kJ/mol).] We calculated the free energy of solvation of Girifalco's fullerene in SPC water using both standard combination rules (results reported above) and the carbon−oxygen Lennard-Jones parameters by Werder et al. The latter decrease the free energy of hydration by approximately 30 kJ/mol, so that the free energy of transfer between octane and water reaches 121 kJ/mol. While this result is still compatible with older estimates for fullerene solubility in water,[56] we notice that an adjustment of the carbon−oxygen parameters seems unnecessary, for two reasons: (1) combination rules provide better agreement with more recent experimental data;[51] (2) the experimental measure of the graphite−water contact angle is subject to a large uncertainty,[55] making it unsatisfactory for use as a target property in force field parametrization. Considering the very good performance of the Girifalco model in all of the properties tested here, we recommend its use in future studies on the C_{60} molecule.

Numerous studies have been carried out on carbon nanoparticles of different sizes and shapes, as well as on functionalized derivatives. It seems likely that the same Girifalco parameters would provide a reasonable description for similar fullerene molecules, such as C_{70}, C_{76}, and C_{84}, although, to the best of our knowledge, validation is lacking. Functionalized fullerenes (with hydroxyl groups, carboxylic acids, metals etc) and carbon nanotubes present significant differences in their electronic structures compared to C_{60}. Use of the Girifalco parameters for those nanoparticles would probably reproduce only qualitatively or semiquantitatively structural and thermodynamic properties of the systems, and careful validation is recommended.

Examining the results on free energies of transfer (Tables 2 and 3), we calculated average errors in atomistic and CG models as the average unsigned difference between calculated and experimental values. The best atomistic model gives an average error of 4.5 kJ/mol, while the MARTINI CG model gives 1.4 kJ/mol. It might appear surprising that the agreement between experimental and calculated free energies of transfer is better with the CG model than with all-atom models. Several considerations can explain this result. First of all, the CG model is parametrized to reproduce those free energies accurately, while only solid-state data were used in the parametrization of the Girifalco model (and no experimental data at all were used in the other all-atom models considered here). Second, the use of geometric combination rules in simulations with a solvent might contribute to the imperfect agreement found here. Arithmetic-mean and geometric-mean combination rules are used in all common all-atom force fields and provide a simple and consistent way to calculate Lennard-Jones parameters for the interaction between different atom types, but they suffer from significant limitations, well-known in the literature.[57] Third, the calculation of free energies of transfer from experimental solubility data involves approximations, as it relies on the assumption of an ideal solution of the monomeric solute and on the assumption and identical solid phases in contact with different solvents. In practice, however, fullerene solutions might very well contain a fraction of (small) fullerene clusters, which alters the free energy of the liquid state. Moreover, solid fullerene is known to form "crystalline solvates" (i.e., solids with intercalated solvent molecules) in the presence of different solvents, leading to differences in the solid phases once they are wet with the solvent.[51] This leads to a significant decrease in solubility, because the crystal solvate is more stable (lower free energy) than the pure, unsolvated crystal. To cope with this problem, Marcus and co-workers calculated "hypothetical solubilities", that take into account the presence of solvates.[51] Results reported in Table 1 are calculated on the basis of hypothetical solubilities in the case of octane. Considering the approximations above, we cannot exclude spurious effects in the interpretation of experimental measures, affecting the reliability of solubility-derived partitioning data. Finally, caution should be used in the interpretation of water-solvent partitioning, as the experimental measure of water solubility is not very precise (due to extremely low solubility of fullerene in water).

In the MARTINI CG force field, as well as in most other CG force fields, Lennard-Jones parameters need to be determined separately for each interaction. In other words, combination rules cannot be used, and there is no simple way of deriving solute−solvent interactions on the basis of solute−solute interactions (nor vice versa). For such coarse-grained models to be accurate in reproducing solute aggregation behavior, it is crucial that a realistic balance be reached between solute−solute interactions and solute−solvent interactions. For example, if solute−solute interactions are overestimated compared to solute−solvent interactions, the solute will be too "sticky". However, the choice of the target property to be used in the optimization of fullerene−fullerene interactions is not trivial. Due to the lower number of particles (and therefore different geometry), coarse-grained models cannot reproduce perfectly the packing of fullerene in FCC crystals; as a consequence, it is very difficult to reproduce accurately the experimental heat of sublimation. In general, the MARTINI force field is not expected to be very accurate in the prediction of solid-state properties.[43] For these reasons, we use primarily the atomistic fullerene−fullerene PMFs as a target in the parametrization of the solute−solute interactions. As for solute−solvent interactions, we use the standard MARTINI procedure (as in our previous work, ref 11), based on matching experimental free energies of transfer between different solvents. The SC4 bead type, used in MARTINI to describe benzene, is used as a starting point in the refinement of the model, both for fullerene−fullerene and for fullerene−solvent interactions. Compared with our previous version,[11] better agreement with experiments is achieved here by careful refinement and by using a larger set of solvents. The bead type with interactions optimized for carbon nanoparticles is coined CNP, and its interactions present small but significant deviations from the interactions of the SC4 bead type. The new model not only yields very good agreement with experimental

free energies of transfer but also reproduces the atomistic dimerization PMF in water within 2.9 kJ/mol and the atomistic dimerization PMF in octane within 0.5 kJ/mol. On the basis of these results, we have reasons to believe that this CG model should be able to reproduce the aggregation behavior of fullerene both in polar and in apolar media.

We compared the performance of our CG model with the one by Chiu and co-workers[58] in terms of partitioning and dimer PMF. Chiu et al.'s CG model predicts significant aggregation of fullerene in lipid membranes.[13] The partitioning behavior of Chiu et al.'s model is qualitatively similar to that of our atomistic and CG models, with a large free energy of transfer from alkane to water (about 80 kJ/mol). The free energy of dimerization in water for the Chiu et al. model is reported to be −20.5 kJ/mol,[58] overestimated (in absolute value) by 5.6 kJ/mol compared to our atomistic calculations. The free energy of dimerization in tridecane is reported to be −8.8 kJ/mol.[58] Li et al. reported a value of −7.1 kJ/mol in the same solvent, using atomistic simulations and 6 ns of sampling per umbrella potential.[54] We ran additional atomistic PMF calculations for the fullerene dimer in tridecane, sampling 100 ns per umbrella potential, and obtained a value of −6.7 (± 0.1) kJ/mol, less favorable than in octane (−7.3 kJ/mol) and consistent with the higher solubility of fullerene in longer alkanes. On the basis of these results, it appears that the free energy of fullerene dimerization in alkanes is too favorable by 2.1 kJ/mol in the Chiu et al. model and too unfavorable by 0.5 kJ/mol in our model. The difference in dimerization free energy between the models will certainly lead to different aggregation behavior and might be sufficient to explain fullerene rapid aggregation in lipid membranes observed by DeVane et al.[13]

PMF calculations of fullerene in a POPC bilayer were used as further validation of the CG model. We notice that, in atomistic simulations, very long sampling was necessary to achieve a statistical uncertainty of about 2 k_BT (200 ns per window, total simulation time of 9.2 μs). This is significantly longer (by over an order of magnitude) compared to previously reported atomistic simulations.[13,21,52] The very slow convergence of the PMF is consistent with recent results by Neale et al., showing that conformational reorganization of the lipid bilayer is the main limiting factor.[59] CG simulations converge more rapidly due to faster membrane dynamics.

The results on the PMFs of fullerene in POPC show very good agreement between atomistic and CG models, with the energy stabilization in the membrane within statistical uncertainty. The difference in the position of the free energy minimum between the atomistic and CG models is due mainly to the greater thickness of the CG POPC membrane relative to the atomistic one. The oleoyl chain in the MARTINI CG model consists of five beads, corresponding to 20 carbon atoms, instead of the 18 carbons of the atomistic model. On the other hand, the (very small) free energy barrier on the permeation path appears to be an artifact of the CG model.

Other CG models of fullerene and carbon nanoparticles have been used in combination with the MARTINI force field for surfactants and lipids. Results from our previous MARTINI CG fullerene model[11] are in reasonable agreement with the present ones. The main difference with the previous model consists in a smaller free energy gain for monomeric fullerene in lipid membranes (∼−80 kJ/mol in the present work, ∼−110 kJ/mol in the old one). The results from the new model are in better agreement with atomistic results reported here, and particularly with fullerene PMF in POPC. Simulations by Bedrov et al.[52] (atomistic) and by DeVane et al.[13] (both atomistic and coarse-grained) also yielded very similar results in terms of fullerene PMF in membranes. Samson and co-workers used fullerene, fullerol, and carbon nanotube CG models to study the interaction of carbon nanoparticles with lipid membranes and detergents.[12,60,61] We notice that they used bead types and interactions from the initial CG model by Marrink (MARTINI v1.0[42]). Also, they chose the most apolar bead type in that force field (equivalent to type C1 in MARTINI v2.0[43]) to represent the carbon nanoparticles. As a result, fullerene stabilization in the center of the membrane was ∼2.5 times larger (about −200 kJ/mol)[12] than the value from atomistic simulations (−80 kJ/mol), indicating that those nanoparticles are too hydrophobic. Kral et al. used MARTINI v2.0[43] and the benzene bead type (SC4) to model nanotubes[62] and graphene[63] interacting with detergents and lipids. While no specific parametrization was carried out in those cases, the choice of the bead type appears reasonable, considering the chemical similarity and the semiquantitative nature of CG models. The SC4 bead type is similar to our CNP bead type (much more than to C1); therefore, we expect the results by Kral and co-workers to be compatible with ours. Within the MARTINI framework, accurate parametrization of nanotubes and graphene appears difficult, due to the scarcity of experimental data on partitioning and solubility of those materials. On the basis of chemical similarity, we suggest that the new CNP bead type should provide qualitatively reasonable predictions in studies of nanotubes and graphene. For more quantitative predictions, tuning and validation of CG parameters against atomistic simulations are recommended.

Considering the overall good performance of the CG model in reproducing experimental partitioning, fullerene−fullerene PMFs, enthalpy of sublimation, and PMF in a membrane, we conclude that the MARTINI model is suitable for the study of the interaction of fullerene with water, organic solvents, and lipid membranes. Using both free energies of transfer and solute−solute PMFs as target properties increases the accuracy of the model, and we suggest that such a parametrization strategy could improve the quality of the MARTINI force field.

AUTHOR INFORMATION

Corresponding Author

*E-mail: luca.monticelli@inserm.fr.

Notes

The authors declare no competing financial interest.

ACKNOWLEDGMENTS

L.M. thanks Emppu Salonen for providing scripts to generate structures for FCC crystals, and for useful discussions. L.M. also thanks Giulia Rossi, Siewert-Jan Marrink, and Peter Tieleman for insightful comments on the manuscript. This work was performed using HPC resources from GENCI-CINES (Grant 2011-076353).

REFERENCES

(1) Kroto, H. W.; Heath, J. R.; Obrien, S. C.; Curl, R. F.; Smalley, R. E. *Nature* **1985**, *318*, 162.

(2) Gust, D.; Moore, T. A.; Moore, A. L. *Acc. Chem. Res.* **2001**, *34*, 40.

(3) Gunes, S.; Neugebauer, H.; Sariciftci, N. S. *Chem. Rev.* **2007**, *107*, 1324.

(4) Sayes, C. M.; Gobin, A. M.; Ausman, K. D.; Mendez, J.; West, J. L.; Colvin, V. L. *Biomaterials* **2005**, *26*, 7587.

(5) Shinohara, H. *Rep. Prog. Phys.* **2000**, *63*, 843.
(6) Gharbi, N.; Pressac, M.; Hadchouel, M.; Szwarc, H.; Wilson, S. R.; Moussa, F. *Nano Lett.* **2005**, *5*, 2578.
(7) Tomanek, D.; Wang, Y.; Ruoff, R. S. *J. Phys. Chem. Solids* **1993**, *54*, 1679.
(8) Wang, Y.; Tomanek, D.; Bertsch, G. F. *Phys. Rev. B* **1991**, *44*, 6562.
(9) Monticelli, L.; Salonen, E.; Ke, P. C.; Vattulainen, I. *Soft Matter* **2009**, *5*, 4433.
(10) Maciel, C.; Fileti, E. E.; Rivelino, R. *J. Phys. Chem. B* **2009**, *113*, 7045.
(11) Wong-Ekkabut, J.; Baoukina, S.; Triampo, W.; Tang, I. M.; Tieleman, D. P.; Monticelli, L. *Nat. Nanotechnol.* **2008**, *3*, 363.
(12) D'Rozario, R. S. G.; Wee, C. L.; Wallace, J. E.; Sansom, M. S. P. *Nanotechnology* **2009**, *20*, 115102.
(13) DeVane, R.; Jusufi, A.; Shinoda, W.; Chiu, C. C.; Nielsen, S. O.; Moore, P. B.; Klein, M. L. *J. Phys. Chem. B* **2010**, *114*, 16364.
(14) Jusufi, A.; DeVane, R. H.; Shinoda, W.; Klein, M. L. *Soft Matter* **2011**, *7*, 1139.
(15) Yannoni, C. S.; Bernier, P. P.; Bethune, D. S.; Meijer, G.; Salem, J. R. *J. Am. Chem. Soc.* **1991**, *113*, 3190.
(16) Jorgensen, W. L.; Maxwell, D. S.; TiradoRives, J. *J. Am. Chem. Soc.* **1996**, *118*, 11225.
(17) Girifalco, L. A. *J. Phys. Chem.* **1991**, *95*, 5370.
(18) Girifalco, L. A. *J. Phys. Chem.* **1992**, *96*, 858.
(19) Rivelino, R.; Maniero, A. M.; Prudente, F. V.; Costa, L. S. *Carbon* **2006**, *44*, 2925.
(20) Qiao, R.; Aluru, N. R. *Nano Lett.* **2003**, *3*, 1013.
(21) Qiao, R.; Roberts, A. P.; Mount, A. S.; Klaine, S. J.; Ke, P. C. *Nano Lett.* **2007**, *7*, 614.
(22) van der Spoel, D.; Lindahl, E.; Hess, B.; van Buuren, A. R.; Apol, E.; Meulenhoff, P. J.; Tieleman, D. P.; Sijbers, A. L. T. M.; Feenstra, K. A.; van Drunen, R.; Berendsen, H. J. C. *GROMACS User Manual*; University of Groningen: Groningen, The Netherlands, 1991.
(23) Weiss, D. R.; Raschke, T. M.; Levitt, M. *J. Chem. Phys. B* **2008**, *112*, 2981.
(24) Jorgensen, W. L.; Madura, J. D.; Swenson, C. J. *J. Am. Chem. Soc.* **1984**, *106*, 6638.
(25) Berendsen, H. J. C.; Postma, J. P. M.; van Gunsteren, W. F.; Hermans, J. In *Intermolecular Forces*; Pullman, B., Ed.; D. Reidel: Dordrecht, The Netherlands, 1981; p 331.
(26) Allen, M. P.; Tildesley, D. J. *Computer Simulation of Liquids*; Oxford University Press: Oxford, U. K., 1987.
(27) Darden, T.; York, D.; Pedersen, L. *J. Chem. Phys.* **1993**, *98*, 10089.
(28) Essmann, U.; Perera, L.; Berkowitz, M. L.; Darden, T.; Lee, H.; Pedersen, L. G. *J. Chem. Phys.* **1995**, *103*, 8577.
(29) Miyamoto, S.; Kollman, P. a. *J. Comput. Chem.* **1992**, *13*, 952.
(30) Hess, B.; Bekker, H.; Berendsen, H. J. C.; Fraaije, J. G. E. M. *J. Comput. Chem.* **1997**, *18*, 1463.
(31) Hess, B. *J. Chem. Theory Comput.* **2008**, *4*, 116.
(32) Parrinello, M.; Rahman, A. *J. Appl. Phys.* **1981**, *52*, 7182.
(33) Van der Spoel, D.; Lindahl, E.; Hess, B.; Groenhof, G.; Mark, A. E.; Berendsen, H. J. C. *J. Comput. Chem.* **2005**, *26*, 1701.
(34) Hess, B.; Kutzner, C.; van der Spoel, D.; Lindahl, E. *J. Chem. Theory Comput.* **2008**, *4*, 435.
(35) Heiney, P. A.; Fischer, J. E.; McGhie, A. R.; Romanow, W. J.; Denenstein, A. M.; McCauley, J. P.; Smith, A. B.; Cox, D. E. *Phys. Rev. Lett.* **1991**, *66*, 2911.
(36) Leach, A. R. *Molecular Modelling: Principles and Applications*, 2nd ed.; Prentice Hall: New York, 2001.
(37) Beutler, T. C.; Mark, A. E.; Vanschaik, R. C.; Gerber, P. R.; Van Gunsteren, W. F. *Chem. Phys. Lett.* **1994**, *222*, 529.
(38) Torrie, G. M.; Valleau, J. P. *J. Comput. Phys.* **1977**, *23*, 187.
(39) Kumar, S.; Bouzida, D.; Swendsen, R. H.; Kollman, P. A.; Rosenberg, J. M. *J. Comput. Chem.* **1992**, *13*, 1011.
(40) Berger, O.; Edholm, O.; Jahnig, F. *Biophys. J.* **1997**, *72*, 2002.
(41) Hub, J. S.; de Groot, B. L.; van der Spoel, D. *J. Chem. Theory Comput.* **2010**, *6*, 3713.
(42) Marrink, S. J.; de Vries, A. H.; Mark, A. E. *J. Phys. Chem. B* **2004**, *108*, 750.
(43) Marrink, S. J.; Risselada, H. J.; Yefimov, S.; Tieleman, D. P.; de Vries, A. H. *J. Phys. Chem. B* **2007**, *111*, 7812.
(44) Monticelli, L.; Kandasamy, S. K.; Periole, X.; Larson, R. G.; Tieleman, D. P.; Marrink, S. J. *J. Chem. Theory Comput.* **2008**, *4*, 819.
(45) Lopez, C. A.; Rzepiela, A. J.; de Vries, A. H.; Dijkhuizen, L.; Hunenberger, P. H.; Marrink, S. J. *J. Chem. Theory Comput.* **2009**, *5*, 3195.
(46) Rossi, G.; Monticelli, L.; Puisto, S. R.; Vattulainen, I.; Ala-Nissila, T. *Soft Matter* **2011**, *7*, 698.
(47) Rossi, G.; Giannakopoulos, I.; Monticelli, L.; Rostedt, N. K. J.; Puisto, S. R.; Lowe, C.; Taylor, A. C.; Vattulainen, I.; Ala-Nissila, T. *Macromolecules* **2011**, *44*, 6198.
(48) Milani, A.; Casalegno, M.; Castiglioni, C.; Raos, G. *Macromol. Theory Simul.* **2011**, *20*, 305.
(49) Chickos, J. S.; Acree, W. E. *J. Phys. Chem. Ref. Data* **2002**, *31*, 537.
(50) Silva Fernandes, F. M. S.; Freitas, F. F. M.; Fartaria, R. P. S *J. Phys. Chem. B* **2004**, *108*, 9251.
(51) Marcus, Y.; Smith, A. L.; Korobov, M. V.; Mirakyan, A. L.; Avramenko, N. V.; Stukalin, E. B. *J. Phys. Chem. B* **2001**, *105*, 2499.
(52) Bedrov, D.; Smith, G. D.; Davande, H.; Li, L. W. *J. Phys. Chem. B* **2008**, *112*, 2078.
(53) Rivelino, R.; Maniero, A.; Prudente, F.; Costa, L. *Carbon* **2006**, *44*, 2925.
(54) Li, L. W.; Davande, H.; Bedrov, D.; Smith, G. D. *J. Phys. Chem. B* **2007**, *111*, 4067.
(55) Werder, T.; Walther, J. H.; Jaffe, R. L.; Halicioglu, T.; Koumoutsakos, P. *J. Phys. Chem. B* **2003**, *107*, 1345.
(56) Korobov, M. V.; Smith, A. L. In *Fullerenes: Chemistry, Physics, and Technology*; Kadish, K. M., Ruoff, R. S., Eds.; Wiley: New York, 2000; p 53.
(57) Halgren, T. A. *J. Am. Chem. Soc.* **1992**, *114*, 7827.
(58) Chiu, C. C.; DeVane, R.; Klein, M. L.; Shinoda, W.; Moore, P. B.; Nielsen, S. O. *J. Phys. Chem. B* **2010**, *114*, 6394.
(59) Neale, C.; Bennett, W. F. D.; Tieleman, D. P.; Pomes, R. *J. Chem. Theory Comput.* **2011**, *7*, 4175.
(60) Wallace, J. E.; Sansom, M. S. P. *Nano Lett.* **2007**, *7*, 1923.
(61) Wallace, J. E.; Sansom, M. S. P. *Nano Lett.* **2008**, *8*, 2751.
(62) Patra, N.; Kral, P. *J. Am. Chem. Soc.* **2011**, *133*, 6146.
(63) Titov, A. V.; Kral, P.; Pearson, R. *ACS Nano* **2010**, *4*, 229.